Robust Neural Networks using Randomized Adversarial Training

Alexandre Araujo, Laurent Meunier, Rafael Pinot, Benjamin Negrevergne

Robust Neural Networks using Randomized Adversarial Training

Alexandre Araujo[1,2*], **Laurent Meunier**[1,3], **Rafael Pinot**[1,4] and **Benjamin Negrevergne**[1]
[1]PSL, Université Paris-Dauphine, Miles Team
[2]Wavestone
[3]Facebook AI Research
[4]CEA, Université Paris-Saclay
{firstname.lastname}@psl.dauphine.eu

Abstract

This paper tackles the problem of defending a neural network against adversarial attacks crafted with different norms (in particular ℓ_∞ and ℓ_2 bounded adversarial examples). It has been observed that defense mechanisms designed to protect against one type of attacks often offer poor performance against the other. We show that ℓ_∞ defense mechanisms cannot offer good protection against ℓ_2 attacks and vice-versa, and we provide both theoretical and empirical insights on this phenomenon. Then, we discuss various ways of combining existing defense mechanisms in order to train neural networks robust against both types of attacks. Our experiments show that these new defense mechanisms offer better protection when attacked with both norms.

1 Introduction

Deep neural networks achieve state of the art performances in a variety of domains such as natural language processing (Radford *et al.*, 2018), image recognition (He *et al.*, 2016) and speech recognition (Hinton *et al.*, 2012). However, it has been shown that such neural networks are vulnerable to *adversarial examples*, i.e. imperceptible variations of natural examples, crafted to deliberately mislead the models (Globerson and Roweis, 2006; Biggio *et al.*, 2013; Szegedy *et al.*, 2014). Since their discovery, a variety of algorithms have been developed to generate adversarial examples (a.k.a. attacks), for example FGSM (Goodfellow *et al.*, 2015), PGD (Madry *et al.*, 2018) and C&W (Carlini and Wagner, 2017), to mention the most popular ones.

Because it is difficult to characterize the space of visually imperceptible variations of a natural image, existing adversarial attacks use surrogates that can differ from one attack to another. For example, Goodfellow *et al.* (2015) use the ℓ_∞ norm to measure the distance between the original image and the adversarial image whereas Carlini and Wagner (2017) use the ℓ_2 norm. When the input dimension is low, the choice of the norm is of little importance because the ℓ_∞ and ℓ_2 balls overlap by a large margin, and the adversarial examples lie in the same space. An important insight in this paper is to observe that the overlap between the two balls diminishes exponentially quickly as the dimensionality of the input increases. For typical image datasets with large dimensionality, the two balls are mostly disjoint. As a consequence, the ℓ_∞-bounded and the ℓ_2-bounded adversarial examples lie in different area of the space, and it explains why ℓ_∞ defense mechanisms perform poorly against ℓ_2 attacks and vice-versa.

We show that this insight is crucial to design defense mechanisms that are robust against both types of attacks, and we advocate for the design of models that incorporate defense mechanisms against both ℓ_∞ and ℓ_2 attacks. Then we evaluate strategies (existing and new ones) to mix up existing defense mechanisms. In particular, we evaluate the following strategies:

(a) *Mixed Adversarial Training* (MAT), a training procedure inspired by *Adversarial Training* (Goodfellow *et al.*, 2015). It is based on augmenting training batches using *both* ℓ_∞ and ℓ_2 adversarial examples. This method defends well against both norms for PGD attacks, but fails against C&W attacks.

(b) *Mixed noise injection* (MNI), a technique that consists in noise injection at test time (Cohen *et al.*, 2019; Pinot *et al.*, 2019). We evaluate different noises and their mixture. This method defends better against C&W attacks, but does not obtain good results against PGD attacks for ℓ_∞ norm.

(c) *Randomized Adversarial Training* (RAT), a solution to benefit from the advantages of both ℓ_∞ adversarial training, and ℓ_2 randomized defense. As we will show, RAT offers the best trade-off between defending against PGD and C&W attacks.

The rest of this paper is organized as follows. In Section 2, we recall the principle of existing attacks and defense mechanisms. In Section 3, we conduct a theoretical analysis to show why the ℓ_∞ defense mechanisms cannot be robust against ℓ_2 attacks and vice-versa. We then corroborate this analysis with empirical results using real adversarial attacks and defense mechanisms. In

*Contact Author

Section 4, we discuss various strategies to mix defense mechanisms, conduct comparative experiments, and discuss the performance of each strategy.

2 Preliminaries on Adversarial Attacks and Defense Mechanisms

Let us first consider a standard classification task with an input space $\mathcal{X} = [0,1]^d$ of dimension d, an output space $\mathcal{Y} = [K]$ and a data distribution $\mathcal{D}$ over $\mathcal{X} \times \mathcal{Y}$. We assume the model f_θ has been trained to minimize a loss function $\mathcal{L}$ as follows:

$$\min_\theta \mathbb{E}_{(x,y)\sim\mathcal{D}} \left[\mathcal{L}(f_\theta(x), y)\right]. \tag{1}$$

In this paper, we consider N-layers neural network models, therefore the model is a composition of N non-linear parametric functions ϕ_{θ_i} (i.e. $f_\theta = \phi^{(N)}_{\theta_N} \circ \cdots \circ \phi^{(1)}_{\theta_1}$).

2.1 Adversarial attacks

Given an input-output pair $(x, y) \sim \mathcal{D}$, an *adversarial attack* is a procedure that produces a small perturbation $\tau \in \mathcal{X}$ such that $f_\theta(x+\tau) \neq y$. To discover the damaging perturbation τ of x, existing attacks can adopt one of the two following strategies: (i) maximizing the loss $\mathcal{L}(f_\theta(x+\tau), y)$ under some constraint on $\|\tau\|_p$, with $p \in \{0, \cdots, \infty\}$ (a.k.a. loss maximization); or (ii) minimizing $\|\tau\|_p$ under some constraint on the loss $\mathcal{L}(f_\theta(x+\tau), y)$ (a.k.a. perturbation minimization).

(i) Loss maximization. In this scenario, the procedure maximizes the loss objective function, under the constraint that the ℓ_p norm of the perturbation remains bounded by some value ϵ, as follows:

$$\operatorname*{argmax}_{\|\tau\|_p \leq \epsilon} \mathcal{L}(f_\theta(x+\tau), y). \tag{2}$$

The typical value of ϵ depends on the value p of the norm $\|\cdot\|_p$ considered in the problem setting. In order to compare ℓ_∞ and ℓ_2 attacks of similar strength, we choose values of ϵ_∞ and ϵ_2 (for ℓ_∞ and ℓ_2 norms respectively) which result in ℓ_∞ and ℓ_2 balls of equivalent volumes. For the particular case of CIFAR-10, this would lead us to choose $\epsilon_\infty = 0.03$ and $\epsilon_2 = 0.8$ which correspond to the maximum values chosen empirically to avoid the generation of visually detectable perturbations. The current state-of-the-art method to solve Problem (2) is based on a projected gradient descent (PGD) (Madry *et al.*, 2018) of radius ϵ. Given a budget ϵ, it recursively computes

$$x^{t+1} = \prod_{B_p(x,\epsilon)} \left(x^t + \alpha \operatorname*{argmax}_{\delta \text{ s.t. } ||\delta||_p \leq 1} \left(\Delta^t | \delta\right) \right) \tag{3}$$

where $B_p(x,\epsilon) = \{x + \tau \text{ s.t. } \|\tau\|_p \leq \epsilon\}$, $\Delta^t = \nabla_x \mathcal{L}\left(f_\theta\left(x^t\right), y\right)$, α is a gradient step size, and $\prod_S$ is the projection operator on S. Both PGD attacks with $p = 2$, and $p = \infty$ are currently used in the literature as state-of-the-art attacks for the loss maximization problem.

(ii) Perturbation minimization. This type of procedures search for the perturbation that has the minimal ℓ_p norm, under the constraint that $\mathcal{L}(f_\theta(x+\tau), y)$ is bigger than a given bound c:

$$\operatorname*{argmin}_{\mathcal{L}(f_\theta(x+\tau),y) \geq c} \|\tau\|_p. \tag{4}$$

The value of c is typically chosen depending on the loss function $\mathcal{L}$. For example, if $\mathcal{L}$ is the $0/1$ loss, any $c > 0$ is acceptable. Problem (4) has been tackled by Carlini and Wagner (2017), leading to the strongest method known so far. (Denoted C&W attack in the rest of the paper.) It aims at solving the following Lagrangian relaxation of Problem (4):

$$\operatorname*{argmin}_\tau \|\tau\|_p + \lambda \times g(x+\tau) \tag{5}$$

where $g(x+\tau) < 0$ if and only if $\mathcal{L}(f_\theta(x+\tau), y) \geq c$. The authors use a change of variable $\tau = \tanh(w) - x$ to ensure that $-1 \leq x + \tau \leq 1$, a binary search to optimize the constant c, and Adam or SGD to compute an approximated solution. The C&W attack is well defined both for $p = 2$, and $p = \infty$, but there is a clear empirical gap of efficiency in favor of the ℓ_2 attack. Accordingly, for this work, we only consider C&W as an ℓ_2 attack solving a norm minimization problem.

2.2 Defense mechanisms

Adversarial Training. *Adversarial Training* (AT) was introduced by Goodfellow *et al.* (2015) and later improved by Madry *et al.* (2018) as a first defense mechanism to train robust neural networks. It consists in augmenting training batches with adversarial examples generated during the training procedure. At each training step, the standard training procedure from Equation 1 is replaced with a $\min\max$ objective function to minimize the expected value of maximum (perturbed) loss, as follows:

$$\min_\theta \mathop{\mathbb{E}}_{(x,y)\sim\mathcal{D}} \left[\max_{\|\tau\|_p \leq \epsilon} \mathcal{L}\left(f_\theta(x+\tau), y\right) \right]. \tag{6}$$

In the case where $p = \infty$, this technique offers good robustness against ℓ_∞ attacks (Athalye *et al.*, 2018). AT can also be performed using other kinds of attacks (including strong ℓ_2 attacks such as C&W albeit at a much higher computational cost). However, as we will discuss in Section 3, ℓ_∞ adversarial training offers poor protection against ℓ_2 adversarial attacks and vice-versa.

Noise injection mechanisms. Another important technique to design robust models against adversarial attacks is to inject noise in the model. Injecting a noise vector η at inference time results in a randomized neural network $\tilde{f}_\theta := f_\theta(x+\eta)$.

In contrast with Adversarial Training, noise injection mechanisms are, in certain cases, provably robust against adversarial examples as discussed by Pinot *et al.* (2019); Cohen *et al.* (2019). Empirical results have also demonstrated their efficiency against ℓ_2 adversarial attacks (Rakin *et al.*, 2018). These works focus however on Gaussian and Laplace distributions a.k.a generalized Gaussian of order 2, and 1 respectively. As the limit of a

generalized Gaussian density (Dytso *et al.*, 2018) when $p \to \infty$ is a Uniform distribution, we also investigate the injection of uniform noise to defend against ℓ_∞ attacks.

3 No Free Lunch for adversarial defenses

3.1 Theoretical analysis

Let us consider a classifier f_{ϵ_∞} equipped with an *ideal defense mechanism* against adversarial examples bounded with an ℓ_∞ norm of value ϵ_∞. It guarantees that for any input-output pair $(x, y) \sim \mathcal{D}$ and for any perturbation τ such that $\|\tau\|_\infty \leq \epsilon_\infty$, f_{ϵ_∞} is not misled by the perturbation (i.e. $f_{\epsilon_\infty}(x+\tau) = f_{\epsilon_\infty}(x)$). We now focus our study on the performance of this classifier against adversarial examples bounded with an ℓ_2 norm of value ϵ_2.

Using Figure 1(a), we observe that any ℓ_2 adversarial example that is also in the ℓ_∞ ball, is guaranteed to be protected by the ℓ_∞ defense mechanism of f_{ϵ_∞}, but not if it is outside the ℓ_∞ ball. To characterize the probability that an ℓ_2 perturbation is guaranteed to be protected by an ℓ_∞ defense mechanism in the general case (i.e. any dimension d), we measure the ratio between the volume of intersection of the ℓ_∞ ball of radius ϵ_∞ and the ℓ_2 ball of radius ϵ_2. As Theorem 1 shows, this ratio depends on the dimensionality d of the input vector x, and rapidly converges to zero when d increases. Therefore a defense mechanism that protects against all ℓ_∞ bounded adversarial examples, is unlikely to be efficient against ℓ_2 attacks.

Theorem 1 (Probability of the intersection goes to 0)**.** *Let $B_{2,d}$, and $B_{\infty,d}$ be two d dimensional balls, respectively for ℓ_2 norm and ℓ_∞ norm. If for all d, one constrains $B_{2,d}$, and $B_{\infty,d}$ to have the same volume, then*

$$\frac{\mathrm{Vol}(B_{2,d} \bigcap B_{\infty,d})}{\mathrm{Vol}(B_{\infty,d})} \to 0 \textit{ when } d \to \infty.$$

Proof. Without loss of generality, let us fix the radius of the ℓ_∞ ball to 1 (denoted $B_{\infty,d}(1)$). One can show that for all d, $\mathrm{Vol}\left(B_{2,d}\left(r_2(d)\right)\right) = \mathrm{Vol}\left(B_{\infty,d}\left(1\right)\right)$. Where $r_2(d) = \frac{2}{\sqrt{\pi}}\Gamma(\frac{d}{2}+1)^{1/d}$, Γ is the gamma function, and $B_{2,d}\left(r_2(d)\right)$ is the ℓ_2 ball of radius $r_2(d)$. Then, thanks to Stirling's formula, $r_2(d) \sim \sqrt{\frac{2}{\pi e}} d^{1/2}$. Finally, if we denote $\mathcal{U}_S$, the uniform distribution on set S, by using Hoeffding inequality between Eq. (9) and (10), we get:

$$\frac{\mathrm{Vol}(B_{2,d}(r_2(d)) \bigcap B_{\infty,d}(1))}{\mathrm{Vol}(B_{\infty,d}(1))} \tag{7}$$

$$= \mathbb{P}_{x \sim \mathcal{U}_{B_{\infty,d}(1)}}\left[x \in B_{2,d}(r_2(d))\right] \tag{8}$$

$$= \mathbb{P}_{x \sim \mathcal{U}_{B_{\infty,d}(1)}}\left[\sum_{i=1}^{d} |x_i|^2 \leq r_2^2(d)\right] \tag{9}$$

$$\leq \exp\left\{-d^{-1}\left(r_2^2(d) - d\mathbb{E}|x_1|^2\right)^2\right\} \tag{10}$$

$$\leq \exp\left\{-\left(\frac{2}{\pi e} - \frac{2}{3}\right)^2 d + o(d)\right\}. \tag{11}$$

Then the ratio between the volume of intersection of the ball and the volume of the ball converges towards 0. □

Theorem 1 states that, when d is large enough, ℓ_2 bounded perturbations have a null probability of being also in the ℓ_∞ ball of the same volume. As a consequence, for any value of d that is large enough, a defense mechanism that offers full protection against ℓ_∞ adversarial examples is not guaranteed to offer any protection against ℓ_2 attacks, and vice-versa[1].

Remark that this result defeats the 2-dimensional intuition: if we consider a 2 dimensional problem setting, the ℓ_∞ and the ℓ_2 balls have an important overlap (as illustrated in Figure 1(a)) and the probability of sampling in the intersection of the two balls is bounded by approximately 98%. However, as we increase the dimensionality d, this probability quickly becomes negligible, even for very simple image datasets such as MNIST. An instantiation of the bound for classical image datasets is presented in Table 1. The probability of sampling in the intersection of the ℓ_∞ and ℓ_2 balls is close to zero for any realistic image setting. In large dimensions, the volume of the corner of the ℓ_∞ ball is much bigger than it appears in Figure 1(a).

Dataset	d	**Inter.** (in $\log_{10}$)
–	2	-0.009
MNIST	784	-144
CIFAR	3072	-578
ImageNet	150528	-28946

Table 1: Bounds of Theorem 1 on the volume of intersection of ℓ_2 and ℓ_∞ balls at equal volume for typical image classification datasets. When $d = 2$, the bound is $10^{-0.009} \sim 0.98$.

3.2 No Free Lunch in practice

Our theoretical analysis shows that if adversarial examples were uniformly distributed in a high dimensional space, then any mechanism that perfectly defends against ℓ_∞ adversarial examples has a null probability of protecting against ℓ_2-bounded adversarial attacks and vice-versa. Although existing defense mechanisms do not necessarily assume such a distribution of adversarial examples, we demonstrate that whatever distribution they use, it offers no favorable bias w.r.t the result in Theorem 1. As we discuss in Sec. 2, there are two distinctive attack settings: loss maximization (PGD) and perturbation minimization (C&W). We analyse the first setting in details and conduct a second series of experiments to demonstrate that the results are similar if we consider the second setting.

Adversarial training vs. loss maximization attacks To demonstrate that ℓ_∞ adversarial training is not robust against PGD-ℓ_2 attacks, we measure the number of ℓ_2 adversarial examples generated with PGD-ℓ_2, lying outside the ℓ_∞ ball. (Note that we consider *all* examples, not just the ones that successfully fool the classifier). To do so, we use the same experimental setting as in Section 4 with ϵ_∞ and ϵ_2 such that the volumes of the two balls are

[1] Th. 1 can easily be extended to any two balls with different norms. For clarity, we restrict to the case of ℓ_∞ and ℓ_2 norms.

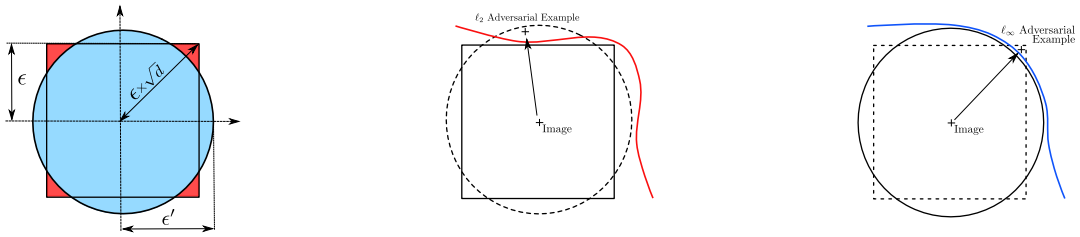

(a) (b) (c)

Figure 1: Left: 2D representation of the ℓ_∞ and ℓ_2 balls of respective radius ϵ and ϵ'. Middle: a classifier trained with ℓ_∞ adversarial perturbations (materialized by the red line) remains vulnerable to ℓ_2 attacks. Right: a classifier trained with ℓ_2 adversarial perturbations (materialized by the blue line) remains vulnerable to ℓ_∞ adversarial examples.

equal. Additionally, we also measure the average ℓ_∞ and ℓ_2 norms of these adversarial examples, to understand more precisely the impact of adversarial training, and we report the accuracy, which reflects the number of adversarial examples that successfully fooled the classifier (cf. Table 2 (top)). The same experiment is conducted for ℓ_2 adversarial training against PGD-ℓ_∞ and the results are presented in Table 2 (bottom). All experiments in this section are conducted on CIFAR-10, and the experimental setting is fully detailed in Section 4.4.

PGD-ℓ_2 vs. $\rightarrow$	**Unprotected**	**AT-ℓ_∞**
Examples inside ℓ_2 ball	100%	100%
Average ℓ_2 norm	0.83	0.83
Examples inside ℓ_∞ ball	0%	0%
Average ℓ_∞ norm	0.075	0.2
Accuracy under attack	0.00	0.37

PGD-ℓ_∞ vs. $\rightarrow$	**Unprotected**	**AT-ℓ_2**
Examples inside ℓ_2 ball	100%	100%
Average ℓ_2 norm	1.4	1.64
Examples inside ℓ_∞ ball	0%	0%
Average ℓ_∞ norm	0.031	0.031
Accuracy under attack	0.00	0.37

Table 2: (Top) number of PGD-ℓ_2 adversarial examples inside the ℓ_∞ and inside the ℓ_2 ball, without and with ℓ_∞ adversarial training. (Bottom) number of PGD-ℓ_∞ adversarial examples inside the ℓ_∞ and inside the ℓ_2 ball, without and with ℓ_2 adversarial training. On CIFAR-10 ($d = 3072$).

The results are unambiguous: *none* of the adversarial examples generated with PGD-ℓ_2 are inside the ℓ_∞ ball (and thus in the intersection of the two balls). As a consequence, we cannot expect adversarial training ℓ_∞ to offer any guaranteed protection against ℓ_2 adversarial examples. We illustrate this phenomenon using Figure 1 (b): notice that the ℓ_2 adversarial example represented in this figure cannot be protected using ℓ_∞ adversarial training which is only designed to push the decision boundary (red line) outside of the ℓ_∞ ball (square), but not outside of the ℓ_2 ball (circle). Our results demonstrate that *all* PGD-ℓ_2 examples are already in this upper area (outside the intersection), before ℓ_∞ adversarial training. Therefore ℓ_∞ adversarial training is unnecessary.

The second experiment naturally demonstrates a similar behaviour. We first observe that adversarial examples generated with PGD-ℓ_∞ lying outside the ℓ_2 ball cannot be eliminated using ℓ_2 adversarial training (as illustrated in Figure 1 (c)). However, Table 2 shows that all examples are already outside the ℓ_2 ball, clustered around the corner of the ℓ_∞ ball (average distance is 1.64 compared to $0.031 \times \sqrt{3072} = 1.71$ for the corner). Therefore, any defense method (including ℓ_2 adversarial training) that would eliminate only adversarial examples inside the ℓ_2 balls, cannot be efficient against ℓ_∞ adversarial examples.

The comparison of accuracy under PGD-ℓ_2 attack of a classifier defended by either ℓ_∞ or ℓ_2 adversarial training corroborate our analysis. In fact, when defended with AT-ℓ_∞ the accuracy of the classifier under attack is 0.37, while the AT-ℓ_2 defends the classifier up to 0.52 i.e. 40% better. Similarly, a classifier defended with AT-ℓ_∞ with an accuracy under PGD-ℓ_∞ attack of 0.43 performs 16% better than the one defended with AT-ℓ_2 which obtains 0.37 accuracy under attack. These results keep confirming our claim: ℓ_2-based defenses are inadequate to defend against ℓ_∞ attacks, and vice-versa.

	Unprotected	**AT-ℓ_∞**
Examples inside intersection	70%	29%
Examples outside intersection	30%	71%
Accuracy under attack	0.00	0.00

Table 3: This table shows the amount of adversarial examples inside the ℓ_∞ ball and inside the ℓ_2 ball but outside the ℓ_∞ ball. We can observe a clear shift between a baseline model (no defense) and a model trained with Adversarial Training PGD ℓ_∞ attacked with C&W attack (Carlini and Wagner, 2017).

Adversarial training vs. perturbation minimization attacks. We now study the performances of an ℓ_2 perturbation maximization attack (C&W) with and without AT-ℓ_∞. It allows us to understand in which area C&W discovers adversarial examples and the impact of AT-ℓ_∞. The results are reported in Table 3. First, when the classifier is undefended, we observe that 70% of adversarial

examples lie inside the intersection of the two balls. This phenomenon is due to the fact that C&W minimizes the ℓ_2 norm of the perturbation. Therefore without AT, the attack is able to discover adversarial examples that are very close to the original image, where the ℓ_∞ and the ℓ_2 balls overlap. When the model is trained with AT-ℓ_∞, we observe a clear shift: 71% of the examples are now outside the ℓ_∞, but still inside the ℓ_2 ball, as illustrated in Figure 1 (b). This means that C&W attack still minimizes the ℓ_2 norm of the perturbation while updating its search space to ignore the examples in the ℓ_∞ ball. Since C&W was always able to discover adversarial examples in this area, AT-ℓ_∞ offers no extra benefit in terms of robustness (0% Accuracy). Together, these results and Theorem 1 confirm that ℓ_∞-based defenses are vulnerable to ℓ_2-based perturbation minimization attacks.

4 Building Defenses against Multiple Adversarial Attacks

So far, we have shown that adversarial defenses are able to protect only against the norm they have been trained on. In order to solve this problem, we propose several strategies to build defenses against multiple adversarial attacks. These strategies are based on the idea that both types of defense must be used simultaneously in order for the classifier to be protected against multiple attacks. In this section we evaluate several of these defense strategies, and compare them against state-of-the-art attacks using a solid experimental setting (the detailed description of the experimental setting is described in Section 4.4).

4.1 MAT – Mixed Adversarial Training

Earlier results have shown that AT-ℓ_p improves the robustness against corresponding ℓ_p-bounded adversarial examples, and the experiments we present in this section corroborate this observation (See Table 4, column: AT). Building on this observation, it is natural to examine the efficiency of Mixed Adversarial Training (MAT) against mixed ℓ_∞ and ℓ_2 attacks. MAT is a variation of AT that uses both ℓ_∞-bounded adversarial examples and ℓ_2-bounded adversarial examples as training examples.

As discussed by Tramèr and Boneh (2019), there are several possible strategies to mix the adversarial training examples. The first strategy (MAT-Rand) consists in randomly selecting one adversarial example among the two most damaging ℓ_∞ and ℓ_2, and to use it as a training example, as described in Equation 12:
MAT-Rand:

$$\min_\theta \mathop{\mathbb{E}}_{(x,y)\sim\mathcal{D}} \left[\mathop{\mathbb{E}}_{p\sim\mathcal{U}(\{2,\infty\})} \left[\max_{\|\tau\|_p \le \epsilon} \mathcal{L}\left(f_\theta(x+\tau), y\right) \right] \right]. \tag{12}$$

An alternative strategy is to systematically train the model with the most damaging adversarial example (ℓ_∞ or ℓ_2). As described in Equation 13:
MAT-Max:

$$\min_\theta \mathop{\mathbb{E}}_{(x,y)\sim\mathcal{D}} \left[\max_{p\in\{2,\infty\}} \max_{\|\tau\|_p \le \epsilon} \mathcal{L}\left(f_\theta(x+\tau), y\right) \right]. \tag{13}$$

The accuracy of MAT-Rand and MAT-Max are reported in Table 4 (Column: MAT). As expected, we observe that MAT-Rand and MAT-Max offer better robustness both against PGD-ℓ_2 and PGD-ℓ_∞ adversarial examples than the original AT does. More generally, we can see that AT is a good strategy against loss maximization attacks, and thus it is not surprising that MAT is a good strategy against mixed loss maximization attacks. However, AT is very weak against perturbations minimization attacks such as C&W, and MAT is no better against such attacks. This weakness makes MAT of little practical use.

4.2 MNI – Multiple Noise Injection

Another important technique to defend against adversarial examples is to use Noise Injection (NI). Pinot *et al.* (2019) demonstrated that injecting noise in the network can give provable defense against adversarial examples. Furthermore, we found that NI offers better protection than AT against perturbation minimization attacks such as C&W, thus, they are good candidates to obtain models robust to multiple attacks. In this work, besides the generalized Gaussian noises, already investigated in previous works, we evaluate the efficiency of uniform distributions which are generalized Gaussian of order ∞. As shown in Table 4 (Columns: NI), noise injection from this distribution gives better results than Gaussian noise injection against all the attacks except PGD-ℓ_∞.

To obtain the best out of both noises, we propose to combine them (MNI) either by convolution (Conv) or by mixture (Mix). Hence, the final noise vector comes from one of the following probability density functions:
MNI-Conv:

$$\frac{1}{\sqrt{2\pi\sigma_1^2}} \exp\left\{\frac{-x^2}{2\sigma_1^2}\right\} * \frac{\mathbb{1}\{|x| \le \sigma_2\}}{2\sigma_2} \tag{14}$$

MNI-Mix:

$$\frac{1}{\sqrt{8\pi\sigma_1^2}} \exp\left\{\frac{-x^2}{2\sigma_1^2}\right\} + \frac{\mathbb{1}\{|x| \le \sigma_2\}}{4\sigma_2}. \tag{15}$$

Following the literature (Pinot *et al.*, 2019), we choose $\sigma_1 = 0.25$. Accordingly, we take $\sigma_2 = 0.2$. The results are presented in Table 4 (Column: MNI). We found that MNI offers comparable results against the experimental setting in (Pinot *et al.*, 2019), but does not improve over NI with a uniform distribution.

4.3 RAT – Randomized Adversarial Training

We now examine the performance of Randomized Adversarial Training (RAT) which mixes Adversarial Training with Noise Injection. We consider the two symmetric settings: RAT-ℓ_∞ and a noise from a normal distribution, as well as RAT-ℓ_2 and a noise from a uniform distribution. The corresponding loss function is defined as follows:

$$\min_\theta \mathop{\mathbb{E}}_{(x,y)\sim\mathcal{D}} \left[\max_{\|\tau\| \le \epsilon} \mathcal{L}\left(\tilde{f}_\theta(x+\tau), y\right) \right]. \tag{16}$$

where $\tilde{f}_\theta$ is a randomized neural network with noise injection as described in Section 2.2.

	Baseline	**AT**		**MAT**		**NI**		**MNI**		**RAT-ℓ_∞**		**RAT-ℓ_2**	
	–	ℓ_∞	ℓ_2	Max	Rand	$\mathcal{N}$	$\mathcal{U}$	Mix	Conv	$\mathcal{N}$	$\mathcal{U}$	$\mathcal{N}$	$\mathcal{U}$
Natural examples	0.94	0.85	0.85	0.80	0.80	0.79	0.87	0.84	0.79	0.74	0.80	0.79	0.87
PGD-ℓ_∞ 20	0.00	0.43	0.37	0.37	0.40	0.23	0.22	0.19	0.20	0.35	0.40	0.23	0.22
PGD-ℓ_2 20	0.00	0.37	0.52	0.50	0.55	0.34	0.36	0.33	0.32	0.43	0.39	0.34	0.37
C&W-ℓ_2 60	0.00	0.00	0.00	0.00	0.00	0.33	0.53	0.41	0.32	0.30	0.41	0.33	0.34
Min Accuracy	0.00	0.00	0.00	0.00	0.00	0.23	0.22	0.19	0.20	**0.30**	**0.39**	0.23	0.22

Table 4: This table shows a comprehensive list of results consisting of the accuracy of several defense mechanisms against ℓ_2 and ℓ_∞ attacks. This table main objective is to compare the overall performance of 'single' norm defense mechanisms (AT and NI presented in the Sec. 2.2) against mixed norms defense mechanisms (MNI, MAT & RAT mixed defenses presented in Sec. 4). The red values present all accuracy *below* 30% which shows that all defense mechanisms have 'weaknesses' with the exception of RAT.

The results of RAT are reported in Table 4 (Columns: RAT-ℓ_∞ and RAT-ℓ_2). We can observe that the first setting offers the best extra robustness, which is consistent with previous experiments, since AT is generally more effective against ℓ_∞ attacks whereas NI is more effective against ℓ_2-attacks. Overall, RAT-ℓ_∞ and a noise from uniform distribution offer the best minimal robustness with at least 0.39 accuracy, 16 points above the second best (NI with noise from a normal distribution, with 0.22).

4.4 Experimental setting

To compare the robustness provided by the different defense mechanisms, we use strong adversarial attacks and a conservative setting: the attacker has a total knowledge of the parameters of the model (white-box setting) and we only consider untargeted attacks (a misclassification from one target to any other will be considered as adversarial). To evaluate defenses based on noise injection, we use *Expectation Over Transformation* (EOT), the rigorous experimental protocol proposed by Athalye *et al.* (2017) and later used by Athalye *et al.* (2018); Carlini *et al.* (2019) to identify flawed defense mechanisms.

To attack the models, we use state-of-the-art algorithms PGD and C&W (see Section 2). We run PGD with 20 iterations to generate adversarial examples and with 10 iterations when it is used for adversarial training. We run C&W with 60 iterations to generate adversarial examples. For bounded attacks, the maximum ℓ_∞ bound is fixed to 0.031 and the maximum ℓ_2 bound is fixed to 0.83. As discussed in Section 2, we chose these values so that the ℓ_∞ and the ℓ_2 balls have similar volumes. Note that 0.83 is slightly above the values typically used in previous publications in the area, meaning the attacks are stronger, and thus more difficult to defend against.

All experiments are conducted on CIFAR-10 with the Wide-Resnet 28-10 architecture. We use the training procedure and the hyper-parameters described in the original paper by Zagoruyko and Komodakis (2016). Training time varies from 1 day (AT) to 2 days (MAT) on 4 GPUs-V100 servers.

5 Related Work

Adversarial attacks have been an active topic in the machine learning community since their discovery (Globerson and Roweis, 2006; Biggio *et al.*, 2013; Szegedy *et al.*, 2014). Many attacks have been developed. Most of them solve a loss maximization problem with either ℓ_∞ (Goodfellow *et al.*, 2015; Kurakin *et al.*, 2016; Madry *et al.*, 2018), ℓ_2 (Carlini and Wagner, 2017; Kurakin *et al.*, 2016; Madry *et al.*, 2018), ℓ_1 (Tramèr and Boneh, 2019) or ℓ_0 (Papernot *et al.*, 2016) surrogate norms.

Defending against adversarial examples is a challenging problem since the number of layers makes it difficult to understand the geometry of the decision boundary. Despite empirically proven efficient, Adversarial training (Goodfellow *et al.*, 2015) gives no formal defense guarantees. Besides this line of work, randomization and smoothing (Xie *et al.*, 2018; Lecuyer *et al.*, 2018; Pinot *et al.*, 2019; Cohen *et al.*, 2019) have gained popularity since they provide guarantees, but so far, the efficiency of these methods remains limited against ℓ_∞-based attacks.

An open question so far is to build an efficient defense against multiple norms. Concurrently to our work, Tramèr and Boneh (2019) proposed to tackle this issue by mixing randomized training with attacks for different norms to defend against multiple perturbations. Then, Salman *et al.* (2019) proposed to mix adversarial training with randomized smoothing to have better certificates against adversarial attacks. These methods are closely related respectively to MAT and RAT. Aside from these similarities, we propose a new geometric point of view for robustness against multiple perturbations, that is backed up theoretically and experimentally. We also conduct a rigorous and full comparison of RAT and MAT as defenses against adversarial attacks. Finally, we propose MNI, that adds mixture of noise to our network and gets promising results. To the best of our knowledge, this is the first work that covers mixtures and convolution of noises with different natures.

6 Conclusion

In this paper, we tackle the problem of protecting neural networks against multiple attacks crafted from different norms. First, we demonstrate that existing defense mechanisms can only protect against one type of attacks. Then we consider a variety of strategies to mix defense mechanisms and to build models that are robust against multiple adversarial attacks. We show that *Randomized Adversarial Training* offers the best global performance.

References

Anish Athalye, Logan Engstrom, Andrew Ilyas, and Kevin Kwok. Synthesizing robust adversarial examples. *arXiv preprint arXiv:1707.07397*, 2017.

Anish Athalye, Nicholas Carlini, and David Wagner. Obfuscated gradients give a false sense of security: Circumventing defenses to adversarial examples. In Jennifer Dy and Andreas Krause, editors, *Proceedings of the 35th International Conference on Machine Learning*, volume 80 of *Proceedings of Machine Learning Research*, pages 274–283, Stockholmsmässan, Stockholm Sweden, 10–15 Jul 2018. PMLR.

Battista Biggio, Igino Corona, Davide Maiorca, Blaine Nelson, Nedim Šrndić, Pavel Laskov, Giorgio Giacinto, and Fabio Roli. Evasion attacks against machine learning at test time. In *Joint European conference on machine learning and knowledge discovery in databases*, pages 387–402. Springer, 2013.

Nicholas Carlini and David Wagner. Towards evaluating the robustness of neural networks. In *2017 IEEE Symposium on Security and Privacy (SP)*, pages 39–57. IEEE, 2017.

Nicholas Carlini, Anish Athalye, Nicolas Papernot, Wieland Brendel, Jonas Rauber, Dimitris Tsipras, Ian Goodfellow, and Aleksander Madry. On evaluating adversarial robustness. *arXiv preprint arXiv:1902.06705*, 2019.

Jeremy M. Cohen, Elan Rosenfeld, and J. Zico Kolter. Certified adversarial robustness via randomized smoothing. *CoRR*, abs/1902.02918, 2019.

Alex Dytso, Ronit Bustin, H. Vincent Poor, and Shlomo Shamai. Analytical properties of generalized gaussian distributions. *Journal of Statistical Distributions and Applications*, 5, 12 2018.

Amir Globerson and Sam Roweis. Nightmare at test time: robust learning by feature deletion. In *Proceedings of the 23rd international conference on Machine learning*, pages 353–360, 2006.

Ian Goodfellow, Jonathon Shlens, and Christian Szegedy. Explaining and harnessing adversarial examples. In *International Conference on Learning Representations*, 2015.

Kaiming He, Xiangyu Zhang, Shaoqing Ren, and Jian Sun. Deep residual learning for image recognition. In *The IEEE Conference on Computer Vision and Pattern Recognition (CVPR)*, June 2016.

Geoffrey Hinton, Li Deng, Dong Yu, George Dahl, Abdelrahman Mohamed, Navdeep Jaitly, Andrew Senior, Vincent Vanhoucke, Patrick Nguyen, Brian Kingsbury, et al. Deep neural networks for acoustic modeling in speech recognition. *IEEE Signal processing magazine*, 29, 2012.

Alexey Kurakin, Ian Goodfellow, and Samy Bengio. Adversarial examples in the physical world. *arXiv preprint arXiv:1607.02533*, 2016.

M. Lecuyer, V. Atlidakais, R. Geambasu, D. Hsu, and S. Jana. Certified robustness to adversarial examples with differential privacy. In *2019 IEEE Symposium on Security and Privacy (SP)*, pages 727–743, 2018.

Aleksander Madry, Aleksandar Makelov, Ludwig Schmidt, Dimitris Tsipras, and Adrian Vladu. Towards deep learning models resistant to adversarial attacks. In *International Conference on Learning Representations*, 2018.

Nicolas Papernot, Patrick McDaniel, Somesh Jha, Matt Fredrikson, Z Berkay Celik, and Ananthram Swami. The limitations of deep learning in adversarial settings. In *Security and Privacy (EuroS&P), 2016 IEEE European Symposium on*, pages 372–387. IEEE, 2016.

Rafael Pinot, Laurent Meunier, Alexandre Araujo, Hisashi Kashima, Florian Yger, Cedric Gouy-Pailler, and Jamal Atif. Theoretical evidence for adversarial robustness through randomization. In *Advances in Neural Information Processing Systems 32*, pages 11838–11848, 2019.

Alec Radford, Jeffrey Wu, Rewon Child, David Luan, Dario Amodei, and Ilya Sutskever. Language models are unsupervised multitask learners. Technical report, OpenAi, 2018.

Adnan Siraj Rakin, Zhezhi He, and Deliang Fan. Parametric noise injection: Trainable randomness to improve deep neural network robustness against adversarial attack. *CoRR*, abs/1811.09310, 2018.

Hadi Salman, Jerry Li, Ilya Razenshteyn, Pengchuan Zhang, Huan Zhang, Sebastien Bubeck, and Greg Yang. Provably robust deep learning via adversarially trained smoothed classifiers. In *Advances in Neural Information Processing Systems*, pages 11289–11300, 2019.

Christian Szegedy, Wojciech Zaremba, Ilya Sutskever, Joan Bruna, Dumitru Erhan, Ian Goodfellow, and Rob Fergus. Intriguing properties of neural networks. In *International Conference on Learning Representations*, 2014.

Florian Tramèr and Dan Boneh. Adversarial training and robustness for multiple perturbations. *arXiv preprint arXiv:1904.13000*, 2019.

Cihang Xie, Jianyu Wang, Zhishuai Zhang, Zhou Ren, and Alan Yuille. Mitigating adversarial effects through randomization. In *International Conference on Learning Representations*, 2018.

Sergey Zagoruyko and Nikos Komodakis. Wide residual networks. *arXiv preprint arXiv:1605.07146*, 2016.